Experimental Neurology 317 (2019) 271–283

Contents lists available at ScienceDirect

Experimental Neurology

journal homepage: www.elsevier.com/locate/yexnr

Research paper

HDAC5 promotes optic nerve regeneration by activating the mTOR pathway

Pita-Thomas Wolfgang[a], Mahar Marcus[a], Joshi Avni[a], Gan Di[a,d,1], Cavalli Valeria[a,b,c,*]

[a] Department of Neuroscience, Washington University School of Medicine, St. Louis, MO 63110, United States of America
[b] Center of Regenerative Medicine, Washington University School of Medicine, St. Louis, MO 63110, United States of America
[c] Hope Center for Neurological Disorders, Washington University School of Medicine, St. Louis, MO 63110, United States of America
[d] Department of Neuroscience, Brandeis University, Waltham, MA 02453, United States of America

ARTICLE INFO

Keywords:
Retinal ganglion cells
Optic nerve regeneration
mTOR
HDAC5
Zymosan

ABSTRACT

Neurons in the central nervous system (CNS) regenerate poorly compared to their counterparts in the peripheral nervous system. We previously showed that, in peripheral sensory neurons, nuclear HDAC5 inhibits the expression of regenerative associated genes. After nerve injury, HDAC5 is exported to the cytoplasm to promote axon regeneration. Here we investigated the role of HDAC5 in retinal ganglion cells (RGCs), a CNS neuron which fails to survive and regenerate axons after injury. In contrast to PNS neurons, we found that HDAC5 is mostly cytoplasmic in naïve RGCs and its localization is not affected by optic nerve injury, suggesting that HDAC5 does not directly suppress regenerative associated genes in these cells. Manipulation of the PKCμ pathway, the canonical pathway that regulates HDAC5 localization in PNS neurons by phosphorylating serine 259 and 498, and other pathways that regulate nuclear/cytoplasmic transport, did not affect HDAC5 cytoplasmic localization in RGC. Also, an HDAC5 mutant whose serine 259 and 488 were replaced by alanine ($HDAC5^{AA}$) to prevent phosphorylation and nuclear export showed a predominantly cytoplasmic localization, suggesting that HDAC5 resides mostly in the cytoplasm in RGCs. Interestingly, expression of $HDAC5^{AA}$, but not HDAC5 wild type, in RGCs in vivo promoted optic nerve regeneration and RGC survival. Mechanistically, we found that $HDAC5^{AA}$ stimulated the survival and regeneration of RGCs by activating the mTOR pathway. Consistently, the combination of $HDAC5^{AA}$ expression and the stimulation of the immune system by zymosan injection had an additive effect in promoting robust axon regeneration. These results reveal the potential of manipulating HDAC5 phosphorylation state to activate the mTOR pathway, offering a new therapeutic target to design drugs that promote axon regeneration in the optic nerve.

1. Introduction

Injuries to the optic nerve caused by ischemic optic neuropathy or glaucoma are followed by retinal ganglion cell (RGC) death and axon degeneration, leading to permanent vision loss (Quigley, 2016). The poor capacity of RGCs to survive and regenerate after injury was first described by Ramon y Cajal (SR, 1913). Over the last few decades, some success has been achieved in promoting axon regeneration and survival of RGCs. For example, inducing an inflammatory response in the retina by injecting zymosan in the eye promotes optic nerve regeneration (Yin et al., 2003). An even larger effect can be achieved when the PI3K/AKT/mTOR pathway is activated by deleting Phosphatase and Tensin homolog (PTEN) or Tuberous Sclerosis Complex 1 (TSC1) (Park et al., 2008; de Lima et al., 2012). However, the number of RGCs responding to these treatments is small, only < 10% of the total RGCs in the retina (Duan et al., 2015; Berry et al., 2019). In addition, overactivation of the mTOR pathway by PTEN deletion causes undesired secondary effects such as an increase in RGC size (Duan et al., 2015) and even cancer (Xie et al., 2015). Therefore, more research is still needed to promote robust optic nerve regeneration without secondary effects.

In contrast to RGCs, peripheral nervous system (PNS) neurons such as dorsal root ganglion (DRG) neurons are able to regenerate their axon following injury, leading to functional recovery. This is in part due to their ability to activate an intrinsic pro-regenerative response (Mahar and Cavalli, 2018). We previously demonstrated a dual role for the class II histone deacetylase 5 (HDAC5) in DRG axon regeneration (Cho and Cavalli, 2012; Cho et al., 2013). The function and localization of HDAC5 is regulated by Protein kinase C subtype μ (PKCμ) and, in some contexts, by Calmodulin Kinase (CamK) (McKinsey et al., 2000). PKCμ is phosphorylated by other PKCs, and achieves full activation when

* Corresponding author at: Department of Neuroscience, 660 South Euclid Avenue, St. Louis, MO 63110, United States of America.
E-mail address: cavalli@wustl.edu (V. Cavalli).
[1] Current address: Department of Biology, Columbia University, New York, NY, USA.

https://doi.org/10.1016/j.expneurol.2019.03.011
Received 10 December 2018; Received in revised form 14 March 2019; Accepted 21 March 2019
Available online 22 March 2019
0014-4886/

serine 916 is phosphorylated, which is a reliable activation marker (Iglesias and Rozengurt, 1998). Activated PKCμ regulates HDAC5 by phosphorylating serine 259 and 498 inducing HDAC5 interaction with 14-3-3 and HDAC5 nuclear export (Vega et al., 2004). On the other hand, phosphorylation of HDAC5 at serine 280 by protein kinase A blocks this interaction and induces nuclear import (Ha et al., 2010). After sciatic nerve injury, a calcium wave induces PKCμ activation in the DRG soma, leading to HDAC5 nuclear export, increased histone acetylation and expression of regenerative associated genes (Cho et al., 2013). In the cytoplasm, HDAC5 also plays an important role for promoting axon growth by regulating the acetylation levels of microtubules (Cho and Cavalli, 2012).

Class I HDACs have been shown to restrict RGCs survival and regeneration after optic nerve injury. A broad histone deacetylases inhibitor, trichostatin A, induces RGC survival after optic nerve crush and expression of the histone acetyltransferase p300 promotes axon regeneration in the optic nerve (Gaub et al., 2011). The dual deletion of HDAC1 and HDAC2 (Lebrun-Julien and Suter, 2015), and the deletion or inhibition of HDAC3 (Schmitt et al., 2014; Schmitt et al., 2018) reduces RGC loss after acute optic nerve injury. These studies suggest that histone deacetylation mediated in part by HDAC3 nuclear accumulation plays a central role in gene silencing and RGCs death after optic nerve injury (Pelzel et al., 2010; Gaub et al., 2011). HDAC3 is known to bind to HDAC5 (Fischle et al., 2002), and HDAC3 re-localizes to the cytoplasm in sensory neurons after sciatic nerve injury (Cho et al., 2013). These studies prompted us to examine the function of HDAC5 in RGCs and manipulate HDAC5 to promote RGC survival and axon regeneration after optic nerve injury.

2. Material and methods

2.1. Mice lines

All animal experiments were performed according to the Washington University animal study guidelines. Animals used in this study include adult and early postnatal Sprague Dawley rats, adult C57Bl/6J mice, adult TSC2 floxed mice (floxed allele; RRID:MGI:3712786) (Hernandez et al., 2007), and adult Raptor floxed mice (floxed allele, MGI:3829755) (Polak et al., 2008).

2.2. Adeno associated vectors and virus

Adenoassociated vector plasmid pscAAV-GFP (Gray and Zolotukhin, 2011) used to generate AAV2-GFP virus was obtained from Addgene (Plasmid #32396). For HDAC5 vector plasmids, GFP from the pscAAV-GFP vector was substituted by the FLAG-HDAC5^{WT}, FLAG-HDAC5^{AA}, or FLAG-HDAC5^{DAD}. The CMV promoter was used in all AAV vectors -based manipulation in this study. AAV2 viral particles were generated by the Viral Core of Washington University. AAV2-Cre was purchased from the viral core of University of North Carolina. Viral titer ranged between 5 × 10^12 vg/mL to 1 × 10^13 vg/mL.

2.3. Retinal ganglion cell purification (adult and early postnatal) and culture

Sprague-Dawley early post−natal pups (P2 − P3) rats were anesthetized by hypothermia and euthanized by decapitation with surgical scissors. Briefly, retinas were dissociated using 16.5 units/mL papain (Worthington) for 30 min. Next, RGCs were purified by immunopanning using antibodies against Anti-Rat Macrophage Polyclonal Antibody (Accurate Chemical) and Thy1 (T11D7 from ATCC), as previously described (Trakhtenberg et al., 2017). RGCs were either lysed with Cytoplasm Extraction buffer (CER) from the nuclear/cytoplasmic fractionation kit (see below) containing protease inhibitors (Roche) and phosphatase inhibitors (Roche). In other experiments, purified RGCs were incubated in an Eppendorf containing 1 mL of media with DMSO, 100 μM of KN-62 (Tocris) and CID755673 (Tocris), or 5 μM I3A (Fisher). After 8 h incubation at 37 °C in rotation, cells were centrifuged and lysed in 80 μL of Cell Lysis buffer (CST) plus protease and phosphatase inhibitors. For some experiments, RGCs were plated on 35 mm tissue culture plates (Falcon) pre coated with poly-D-lysine (PDL; 10 mg/mL; Sigma) and laminin (1 mg/mL; Life Technologies). RGCs were cultured in defined growth medium consisting of Neurobasal media (Life Technologies) supplemented with sodium pyruvate, *N*-acetyl cysteine, insulin, BDNF, CNTF, and GS21 supplement medium. In some experiments, forskolin (5 μM; Sigma) or leptomycin (20 ng/mL; Sigma) was added to the medium, and after 24 h cells were washed three times with PBS and lysed in 100 μL of Cell Lysis buffer (CST), using a cell scraper (Falcon). For immunostaining, RGCs were plated on glass bottom dishes (MatTek) also coated with poly-D-lysine and laminin. After 24 h, cells were fixed for 30 min in 4% paraformaldehyde in the same plate followed by three PBS washes.

2.4. Adult skeletal muscle cell purification

Adult Skeletal Muscle Myofibers were purified as previously described (Pasut et al., 2013). Briefly, Extensor Digitorum Longus muscle of adult mice was dissected and incubated in 1.5 mg/mL collagenase (C6885; Sigma) in DMEM until the muscle started to loosen up. Then digested muscle is transferred to a new dish where tissue is flushed with warm medium until myofibers are released from the muscle. Using a pipette, myofibers are transferred to a 1.5 mL tube and centrifuged at low speed. The supernatant was discarded and nuclear/cytoplasmic fractionation was performed.

2.5. Rodent surgeries

All surgical procedures were performed under isofluorane anesthesia and approved by Washington University in St. Louis, School of Medicine Animal Studies Committee.

Intravitreal injection was performed as previously described with minor modifications (Steketee and Goldberg, 2012). One drop of atropine solution (1%; Akorn) was applied topically to dilate the pupils. A fine tip of pulled glass micropipette was attached to a Hamilton syringe using a needle compression fitting (55750-01; Hamilton), and loaded with 1.25 μL of adeno-associated virus (AAV2) or 594 fluorescently labeled cholera toxin B (Life Technologies). The tip was then inserted through the sclera with a 45° angle and the solution was slowly released in the vitreal space.

Optic nerve crush was performed as previously described with minor modifications (Ban et al., 2017). Investigator performing the surgery was blinded to the treatments. One hour before surgery, Buprenorphine (1.0 mg/kg) was injected subcutaneously. Animals were then anesthetized with isofluorane and 5% Sodium Chloride eye drops were applied preoperatively to protect the cornea during surgery. Left optic nerve was exposed intraorbitally and crushed with sterile jeweler's forceps for 3 s around 1 mm behind the optic disc. To preserve the retinal blood supply, care was taken not to damage the underlying ophthalmic artery. The endpoint of this surgery was between 1 and 28 days.

In some experiments, eye tissues were harvested for biochemical purposes. After sacrificing the animal, the eye together with the proximal part of the optic nerve was dissected out. The retina was extracted by cutting out the sclera and the cornea. The proximal part to the injury site was also resected. Tissue was then transferred to a 1.5 mL tube containing 80 μL of either Cell Lysis Buffer (Cell Signaling Technology) or CER buffer plus protease inhibitor and phosphatase inhibitors (Roche), and homogenized using disposable pestles and a pestle motor (Kontes).

In another set of experiments, rapamycin was prepared according to Chen et al. (Chen et al., 2009). Briefly, Rapamycin (LC Laboratories) was resuspended in ethanol at 50 mg/mL and then diluted in 5%

Tween-80 (Sigma) and 5% PEG-400 (Sigma) to a working solution of 1 mg/mL. Mice received 6 mg/kg every other day by intraperitoneal injection. Vehicle solution without rapamycin was injected in control animals.

2.6. Nuclear/cytoplasmic fractionation

Nuclear and cytoplasmic fractionation was performed using NE-PER Nuclear and Cytoplasmic Extraction Reagents (Thermo Scientific). Briefly, homogenized cells or retinas in CER buffer were vortexed for 10 s and centrifuged at 12,000 ×*g* at 4 °C for 30 min. Supernatant was collected and stored at −80 °C while the pellet was washed once with PBS and then resuspended in Nuclear Extraction buffer or RIPA buffer to extract nuclear proteins.

2.7. Immunoprecipitation

Immunoprecipitation was performed using anti-flag antibody attached to protein G beads. Nuclear and cytoplasmic fractions obtained from one retina were diluted three times with water/0.02% tween and PBS/0.02% tween respectively. Next, 10 µL of anti-flag beads were resuspended in each of these samples, and incubated overnight at 4 °C in a rotary shaker. Beads were separated using a magnet and washed three times with PBS/0.02% tween, transferred to a new tube, and boiled in 1× Laemmli Buffer for 5 min. Beads were discarded and the supernatant was loaded in an electrophoresis followed by a western blot.

2.8. Electrophoresis and western blot

For western blot, 5× SDS loading buffer, prepared according to Cold Spring Harbor protocols, was added to samples. These samples were heated at 95 °C for 5 min and, after cooling down on ice were run in on 8–16% NuPAGE SDS-PAGE gradient gel (Life Technologies) in MOPS SDS Running Buffer (Life Technologies), and transferred to 0.2 µm nitrocellulose membranes (Amersham). Next, these membranes were blocked in blocking buffer (3% BSA in 0.1% Tween-20 at pH 7.6 for 1 h, and incubated at 4 °C overnight in blocking buffer with 1:1000 primary antibodies, such as monoclonal anti-HDAC5 antibody (H4538; Sigma), monoclonal anti-phosphorylated (Ser 498) HDAC5 (sc101692; Santa Cruz), rabbit anti-HDAC3 antibody (sc11417; Santa Cruz), rabbit anti-Histone3 antibody (9715S; CST), rabbit anti-GAPDH antibody GAPDH (sc25778, Santa Cruz), rabbit anti-Phospho-PKCµ Ser916 (2051S; CST), rabbit anti-PKCµ (2052S; CST), rabbit anti-phospho-c-Jun antibody (9261 s; CST), goat anti-Brn3a (sc-31984; Santa Cruz), and rabbit anti-β3 tubulin antibody (PRB-435P, Covance). Membranes were then washed in TBST 3 times, incubated with horseradish peroxidase (HRP)-conjugated anti-rabbit or anti-mouse IgG (1:5000; Invitrogen) for 1 h at room temperature, washed in TBST three times, and developed with SuperSignal West Dura Chemiluminescent Substrate (Thermo Scientific). The membranes were imaged using ChemiDoc System (Bio Rad) and analyzed with ImageLab software.

2.9. Perfusion and cryostat sectioning

Mice were sacrificed by CO_2 asphyxiation and then perfused with 15 mL of PBS followed by 15 mL of paraformaldehyde 4%. Eyes and optic nerve were dissected out and an incision was made in the cornea. These tissues were then fixed for 3 h in 4% paraformaldehyde, washed 3 times in PBS, and incubated in 30% sucrose in PBS at 4 °C overnight. Optic nerves were separated from the retina using spring scissors, embedded in tissue tek and directly sectioned at 11 µm in a Cryostat. Eyes were embedded in tissue-tek and frozen at −80 °C, and then sectioned at 11 µm thickness. Cryosections were always mounted on Superfrost Plus micro slides (Fisherbrand).

2.10. Immunohistochemistry and quantitative analysis

Cryosections or fixed cells were blocked with 20% goat serum plus 0.2% Triton X-100 in PBS for 1 h. Next, these sections were incubated overnight at 4 °C in the same buffer containing primary antibodies goat anti-Brn3a (sc-31984; Santa Cruz) or monoclonal anti-Brn3a (sc-8429; Santa Cruz), rabbit anti-pS6 (Ser240/244) antibody (5364S; CST), rabbit anti-β3 tubulin antibody (PRB-435P, Covance). Then, samples were washed 3 times in PBS, incubated h with DAPI (1:3000, Life Technologies) and Alexa fluorophore-conjugated secondary antibodies (1:500, Life Technologies) in PBS for 2h at 4C, washed three times in PBS and mounted in ProLong Gold (P36934, Life Technologies) with a glass coverslip. Last, samples were imaged using a Nikon TE-2000E fluorescence microscope and analyzed in FIJI (NIH). For survival analysis, investigator performing the quantification was blinded to the treatments. Number of $Brn3a^+$ cells per section was counted and normalized to the total length of the RGC layer of that section. Three to four sections per retina were counted.

For optic nerve regeneration analysis, the investigator performing the quantification was blinded to the treatments. Lines at 250, 500, 750 and 1000 µm were drawn using FIJI, and the number of $CTXB^+$ segments contacting the lines were counted. Three to four sections were averaged to obtain the average number of regenerating axons/mm. The number of regenerating axons was estimated using the formula previously described (Park et al., 2008) with minor modifications: 2π x optic nerve radius x [average axons/µm]/11.

2.11. RNA-seq

To isolate the RNA for sequencing, retinas were dissected from four female C57Bl/6 J per condition, and homogenized in 300 µl lysis buffer using disposable pestles attached to a motor (Kontes). RNA was purified using the PureLink RNA Mini kit with on column DNase treatment and submitted to Washington University Genome Technology Access Center for quality control, library preparation, and sequencing. Briefly, RNA was quality controlled and quantified using both a Nanodrop 2000 and an Agilent Bioanalyzer; all samples passed quality control (RIN > 8, A260/268 > 2). Next, rRNA was depleted using a Ribo-Zero rRNA removal kit, cDNA libraries were generated using a Clontech SMARTer kit, and libraries were sequenced on an Illumina HiSeq3000 using 1 × 50 lanes. Quality control was then performed on fastq files using FastQC and reads aligned to mm10 using STAR-align. Next, aligned reads were counted using HTseq-count and differential expression determined using DESeq2. Genes with fewer than an average of 5 counts per million were removed from the analysis. RNA-seq FastQ files were deposited at the NCBI GEO database (http://www.ncbi.nlm.nih.gov). Accession number GSE120257.

2.12. Experimental design and statistical analysis

In the experiments where western blot statistical analysis was performed, at least three female C57BL/6J mice or female Sprague Dawley rats were used per condition. Bands were quantified using Image Lab software and One-way ANOVA analysis was performed using Statistica 7 software.

For optic regeneration experiments, four to seven C57BL/6J female mice were used per condition in each experiment. However, in the experiments performed in TSC2 floxed mice, the number of animals was reduced to three and four per condition and mice were used regardless of their sex. The reason was that littermates were preferred in this experiment to reduce variability and therefore the litter size of this particular mice line was a limiting factor. In experiments comparing different HDAC5 mutants, four experiments performed on different days were combined. In each of these experiments, an AAV-GFP control was always included. One-way ANOVA with Bonferroni post hoc analysis was performed using Statistica 7 software, similar to previously

reported (Park et al., 2008).

In the in vivo RGC survival assay and in the quantifications of the percentage of $pS6^+$ RGCs, five C57BL/6J female mice were used per condition. One-way ANOVA with Tukey's post hoc test analysis was performed using Statistica 7 software similarly to previously reported (Li et al., 2016).

For RNAseq, principal component analysis was then performed to detect outliers. Due to this, one of the GFP samples was removed. A cutoff of a *p*-adjusted value of .1 was used to identify differentially expressed genes. Downstream analysis of biological and signaling pathways was performed using MetaCore using a *p*-value of .05 to determine enriched pathways.

3. Results

3.1. HDAC5 is largely cytoplasmic in naïve and injured RGCs

We have previously shown that the localization of HDAC5 is critical for its effects in axon regeneration in DRG neurons (Cho et al., 2013). Therefore, we first determined the localization of HDAC5 in naïve RGCs and in RGCs after optic nerve injury. Acutely purified RGCs by immunopanning represent a pure population, with more than > 98% of the cells positive for the RGC marker Brn3a (Fig. 1A), as previously reported (Barres et al., 1988). Nuclear and cytoplasmic fractionation of these acutely purified RGCs followed by western blot analysis revealed that HDAC5 is largely found in the cytoplasm, whereas HDAC3 is equally distributed in both fractions (Fig. 1B).

Since, it has been reported that injury induces a widespread silencing of genes in RGCs mediated in part by HDAC3 nuclear import (Pelzel et al., 2010), we asked whether HDAC5 also translocates to the nucleus after injury. We performed an optic nerve crush (ONC) and isolated retinas at various days after injury (Fig. 1C). We observed that PKCμ activation is not increased (One-way ANOVA $F(3, 8) = 0.32$, $p = .80$) and HDAC5 phosphorylation at serine 498 does not increase (One-way ANOVA $F(5, 6) = 0.37$, $p = .85$) at 2, 5 or 8 days post injury (Fig. 1D, E and F), suggesting that HDAC5 is not regulated by PKCμ phosphorylation in the retina after axon injury. Consistent with this result, nuclear fractionation showed that HDAC5 remains largely cytoplasmic in both control and injured retinas (Fig. 1G). In contrast, HDAC3 was detected in both the nuclear and cytoplasmic fractions, but we did not observe HDAC3 nuclear accumulation after injury (Fig. 1G). Additionally, and in contrast to what we have reported in sciatic nerve (Cho et al., 2013), we did not observe an accumulation of HDAC5 (One-way ANOVA $F(1, 5) = 0.009$, $p = .92$) or an activation of PKCμ (One-way ANOVA $F(1, 5) = 0.09$, $p = .76$) in the proximal site of the injured optic nerve (Fig. 1H and I). Finally, we overexpressed FLAG-tagged $HDAC5^{WT}$ in RGCs in vivo using adeno-associated virus (AAV2) intravitreal injection, and immunoprecipitated FLAG-$HDAC5^{WT}$ from control and injured retinas. We found that FLAG-$HDAC5^{WT}$ is also localized in the cytoplasm and that injury does not change HDAC5 localization (Fig. 1K). These results indicate that HDAC5 is largely cytoplasmic in RGCs and that optic nerve injury does not change its localization.

3.2. HDAC5 subcellular localization in RGCs is not regulated by canonical signaling pathways

Next, we determined whether HDAC5 phosphorylation state has an effect on its cellular localization in RGCs. Since both PKCμ and CamK phosphorylate HDAC5 at serines 259 and 498 to promote its nuclear export in myocytes (McKinsey et al., 2000; Vega et al., 2004), we asked whether inhibiting PKCμ and CamK by incubating RGCs with their respective inhibitors CID755673 and KN62 prevent HDAC5 nuclear export. We found that these drugs clearly reduced the phosphorylation levels of HDAC5 at Serine 498 (Fig. 2A), but the cytoplasmic localization of HDAC5 did not change (Fig. 2B). To further support that HDAC5 phosphorylation at serines 259 and 498 does not induce HDAC5 nuclear export in RGCs, we overexpressed $HDAC5^{WT}$ and two other constructs of HDAC5 that mimic the phosphorylation states of HDAC5 in RGCs (Fig. 2C). In one construct, serine 259 and 498 were substituted with alanine ($HDAC5^{AA}$) to prevent phosphorylation. This mutation blocks interaction with the 14-3-3 protein (Vega et al., 2004), and prevents nuclear export in myocytes. In another, construct serine 259 and 498 were substituted with aspartic acid to mimic phosphorylation and serine 280 substituted with alanine to prevent phosphorylation by PKA ($HDAC5^{DAD}$). $HDAC5^{DAD}$ interact with 14-3-3 to be transported to the cytoplasm in myocytes (Ha et al., 2010). All three constructs, expressed at similar levels in RGCs in vivo using AAV2 intravitreal injection, were predominantly cytoplasmic (Fig. 2D). We also expressed these HDAC5 constructs in cultured RGCs and confirmed that both $HDAC5^{DAD}$ and $HDAC5^{AA}$ were predominantly in the cytoplasm (Fig. 2E). These results suggest that the canonical pathways regulating HDAC5 localization (Vega et al., 2004) are not involved in HDAC5 subcellular localization in RGC.

To further support that in RGCs, HDAC5 is insensitive to canonical signals that in other cell types regulate its localization, we treated RGCs with two drugs that have been previously demonstrated to promote HDAC5 nuclear localization, forskolin (Ha et al., 2010) and leptomycin (Harrison et al., 2004). Neither forskolin, which activates PKA and phosphorylates HDAC5 serine 280 in cardiomyocytes (Ha et al., 2010), nor leptomycin, which inhibits nuclear export of proteins, were able to induce HDAC5 nuclear localization in RGCs (Fig. 2F). As a control, we used purified adult skeletal muscle cells (ASM), a cell type in which HDAC5 nuclear localization is known to inhibit genes for muscle growth (Liu et al., 2009), and in which we clearly observed HDAC5 localization in both the cytoplasmic and nuclear fraction (Fig. 2F). These results further support the notion that HDAC5 is largely cytoplasmic in RGCs.

3.3. $HDAC5^{AA}$ activates mTOR and increases optic nerve regeneration and survival of injured RGCs

Because mutation of HDAC5 phosphorylation was shown to affect interactions with other proteins in addition to regulate subcellular localization (Greco et al., 2011), we tested if overexpressing $HDAC5^{WT}$ and HDAC5 mutants in RGCs in vivo has an effect on axon regeneration (Fig. 3A). $HDAC5^{WT}$ and $HDAC5^{DAD}$ behaved similarly and were not significantly different than the control GFP virus, in which very limited axon growth past the injury site was observed (Fig. 3B and C). However, $HDAC5^{AA}$ promoted optic nerve regeneration (One-way ANOVA $F(8, 68) = 5.03$, $p = .00006$ with Bonferroni's post hoc test), doubling the number of regenerating axons at all distances past the injury site (Fig. 3B and C). Therefore, although the localization of $HDAC5^{AA}$ and $HDAC5^{DAD}$ is indistinguishable using nuclear fractionation, their effects in optic nerve regeneration are very different.

It is well established that activating mTOR by deleting TSC1, TSC2 (Park et al., 2008; Abe et al., 2010) or PTEN (Park et al., 2008; Christie et al., 2010) promotes axon regeneration. In RGC, these manipulations not only promote optic nerve regeneration but also RGC survival, by blocking the injury-induced dephosphorylation of the S6 ribosomal protein (S6) after optic nerve crush (Park et al., 2008). Since it has recently shown that, in a hypothalamic cell line, cytoplasmic HDAC5 can indirectly regulate mTOR activation (Ma et al., 2015), we tested if $HDAC5^{AA}$ activates the mTOR pathway to promote RGC survival and regeneration. We observed a 10% increase in the number of surviving RGCs (labeled with the nuclear marker Brn3a) after injury in retinas overexpressing $HDAC5^{AA}$ compared to the other treatments (One-way ANOVA $F(2, 12) = 13.38$, $p = .00089$ with Tukey's post hoc test; $p = .004$ vs GFP and $p = .001$ vs $HDAC5^{DAD}$ but not difference ($p = .75$) between $HDAC5^{DAD}$ and GFP) (Fig. 3D and E). We also observed a higher percentage of cells labeled with phosphorylated S6 (pS6) in the surviving RGCs in retinas expressing $HDAC5^{AA}$ compared

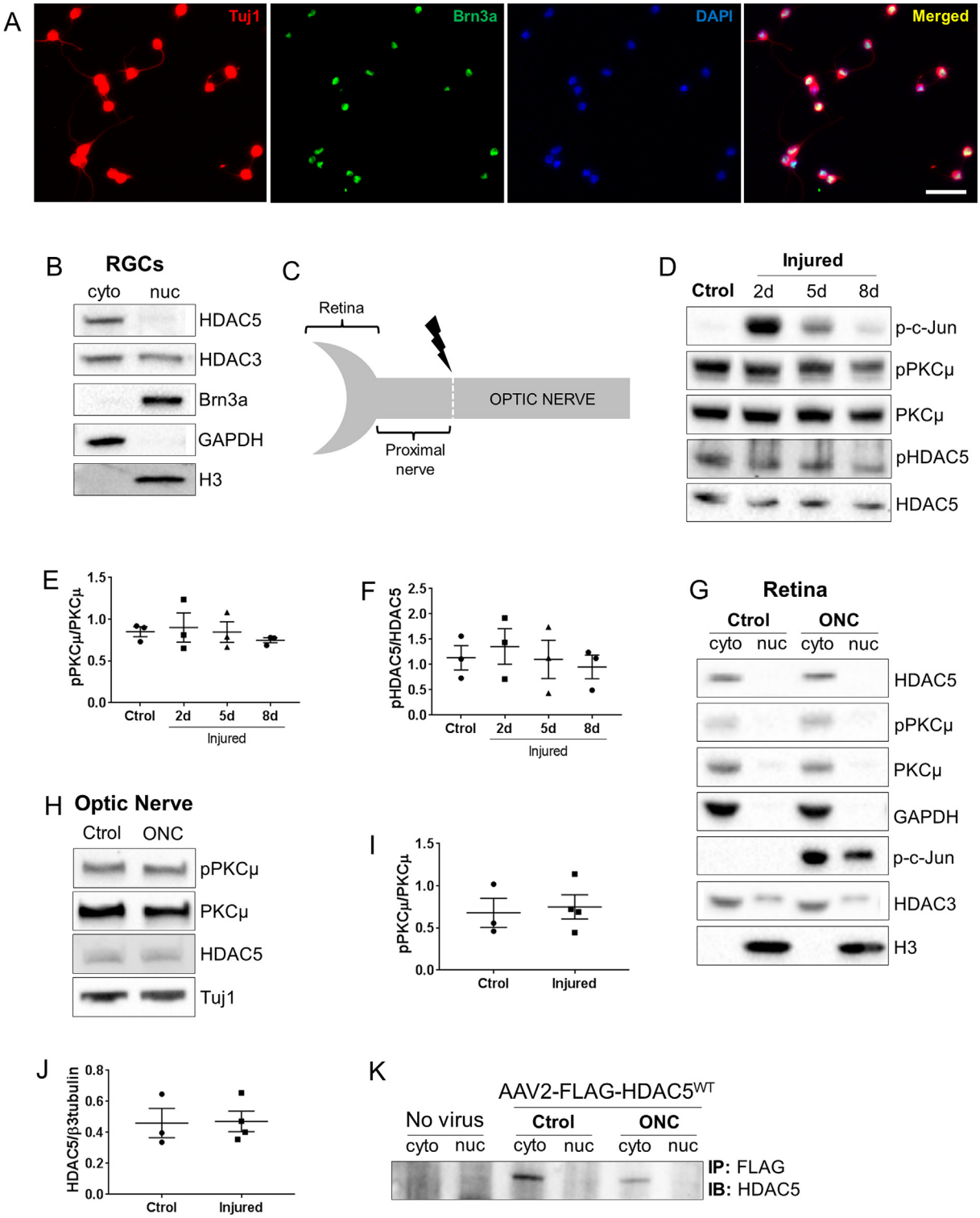

Fig. 1. HDAC5 is predominantly localized in the cytoplasm of RGCs and does not change its location after injury.
(A) Rat RGC cultures purified by immunopanning and stained with β3-tubulin (cytoplasm, red), Brn3a (nuclei, green), and DAPI (nuclei, blue), show that the majority of cells are triple positive, demonstrating the high purity of the culture. (B) Immunoblot for nuclear (nuc) and cytoplasmic (cyto) fractions of early postnatal rat purified RGCs shows that HDAC5 is predominantly in the cytoplasm. (C) Diagram showing the eye and optic nerve regions dissected for following immunoblot analyses. (D) Immunoblot of mouse retina extracts isolated at 2, 5, and 8 days after optic nerve injury. (E) Quantification of (D) shows that there is no difference in the phosphorylation levels of PKCμ (serine 916) after optic nerve injury. (F) Quantification of (D) showing that there is no difference in the phosphorylation levels of HDAC5 (serine 498) after optic nerve injury. (G) Immunoblot of nuclear (nuc) and cytoplasmic (cyto) fractions of mouse uninjured retinas and retinas 2 days after optic nerve injury. (H) Immunoblot of the region proximal to the injury site 2 days after optic nerve injury in rats. (I) Quantification of (H) showing that there is no difference in the phosphorylation levels of PKCμ (serine 916) after optic nerve injury. (J) Quantification of (H) showing that there is no difference in the accumulation of HDAC5. (K) FLAG immunoprecipitation followed by immunoblot for HDAC5 in retinas infected with AAV2 virus encoding FLAG-HDAC5^{WT}, uninjured and 2 days after optic nerve injury. Plotted values in (E), (F), (J) and (I) were quantified and expressed as mean ± SEM. Scale bar = 50 μm. Statistical analysis is a One-way ANOVA. N at least 3 in B, D, G, and L. (For interpretation of the references to colour in this figure legend, the reader is referred to the web version of this article.)

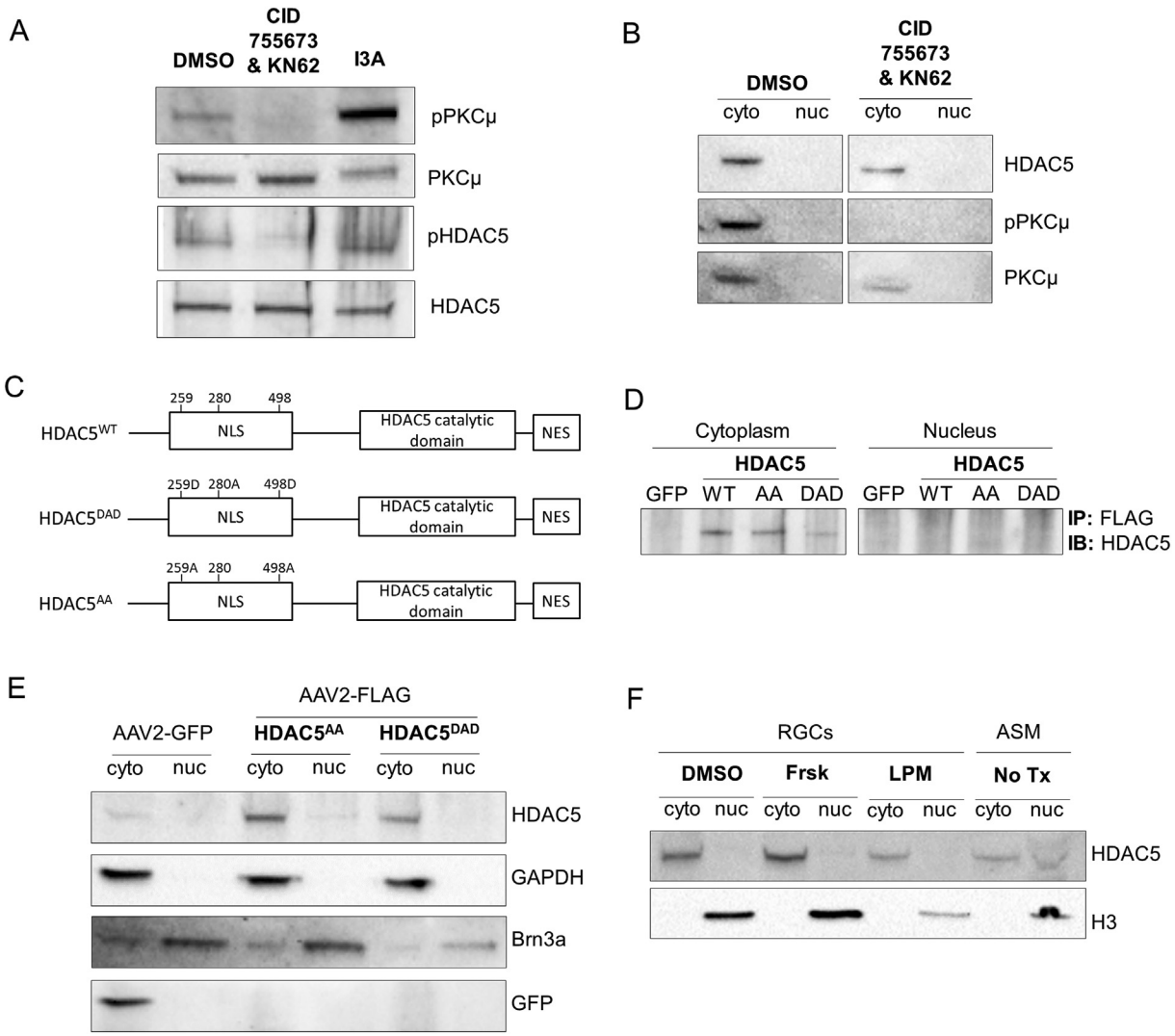

Fig. 2. The cytoplasmic localization of HDAC5 is independent of the phosphorylation states of key serines 259, 280, 498.
(A) Immunoblot of cultured rat RGCs treated for 8 h with vehicle (DMSO), 100 μM CID755673 + 100 μM KN62, or 1 μM I3A. (B) Immunoblot for nuclear (nuc) and cytoplasmic (cyto) fractions of cultured rat RGCs treated for 8 h with vehicle (DMSO), or 100 μM CID755673 + 100 μM KN62. (C) Diagram of the HDAC5 constructs, $HDAC5^{WT}$, $HDAC5^{AA}$, and $HDAC5^{DAD}$, showing the serines that are substituted for alanine (A, phospho-dead) or aspartic acid (D, phospho-mimic), NLS, nuclear localization signal region, NES, nuclear export signal region. (D) FLAG immunoprecipitation followed by immunoblot for HDAC5 in retinas infected with AAV2 encoding GFP, FLAG-$HDAC5^{WT,}$ FLAG-$HDAC5^{AA}$, or FLAG-$HDAC5^{DAD}$ 15 days prior to sacrifice. (E) Immunoblot for nuclear (nuc) and cytoplasmic (cyto) fractions of cultured rat RGCs infected with AAV2-GFP, AAV2-FLAG-$HDAC5^{AA}$, or AAV2-FLAG-$HDAC5^{DAD}$ 8 days prior to harvest. (F) Immunoblot for nuclear (nuc) and cytoplasmic (cyto) fractions of cultured rat RGCs treated for 24 h with vehicle (DMSO), forskolin (frsk), or leptomycin (LPM). As a positive control for nuclear HDAC5, myofibers from adult skeletal muscle (ASM) were used. $N = 3$ in B and C, and $n = 2$ in D.

to retinas expressing GFP or $HDAC5^{DAD}$ (One-way ANOVA $F(2, 9) = 25.56$, $p = .00019$ with Tukey's post hoc test; $p = .003$ vs GFP and $p = .02$ vs DAD) (Fig. 3D and F and C). We also observed a slight but significant increase in the number of pS6 positive RGCs in retinas expressing $HDAC5^{DAD}$ compared to GFP ($p = .011$). These results suggest that HDAC5 is able to regulate mTOR activity but that $HDAC5^{DAD}$ is less efficient than $HDAC5^{AA}$ and is unable to promote survival or axon regeneration of RGCs.

3.4. HDAC5 regulates the expression of genes in the PI3K-mTOR pathway

To determine the underlying gene expression changes leading to the phenotypical differences in optic nerve regeneration between control GFP, $HDAC5^{DAD}$, and $HDAC5^{AA}$ we performed an RNAseq analysis. Whole retina were collected 4 days after ONC in animals injected with AAV2 two weeks before ONC, and compared them with non-injected/non-injured retinas. Since ~70% of cells transduced by intravitreal injection of AAV2 are RGCs (Harvey et al., 2002), most gene expression changes between conditions should reflect changes occurring in RGCs, or changes in other cells as a result of $HDAC5^{AA}$ and $HDAC5^{DAD}$ expression in RGCs. As expected, we observed that retinas expressing $HDAC5^{AA}$ and $HDAC5^{DAD}$ showed 20% more total HDAC5 compared to GFP expressing retina (Fig. 4A). To differentiate between endogenous HDAC5 and overexpressed HDAC5, we focused our analysis in the HDAC5 region around amino acid 498, where the mutations of these two constructs reside. We were able to detect these mutations and compared their expression levels to endogenous HDAC5, confirming that both mutated versions were expressed at similar levels (Fig. 4B). Next, we identified the genes that are differentially expressed in GFP, $HDAC5^{DAD}$, and $HDAC5^{AA}$ compared to uninjured, uninjected controls, and found that a large proportion of the genes differentially expressed are shared between the three conditions (Fig. 4C), indicating common genes affected by injury and AAV injection. We also observed that $HDAC5^{DAD}$ and $HDAC5^{AA}$ differentially regulated a specific set of genes

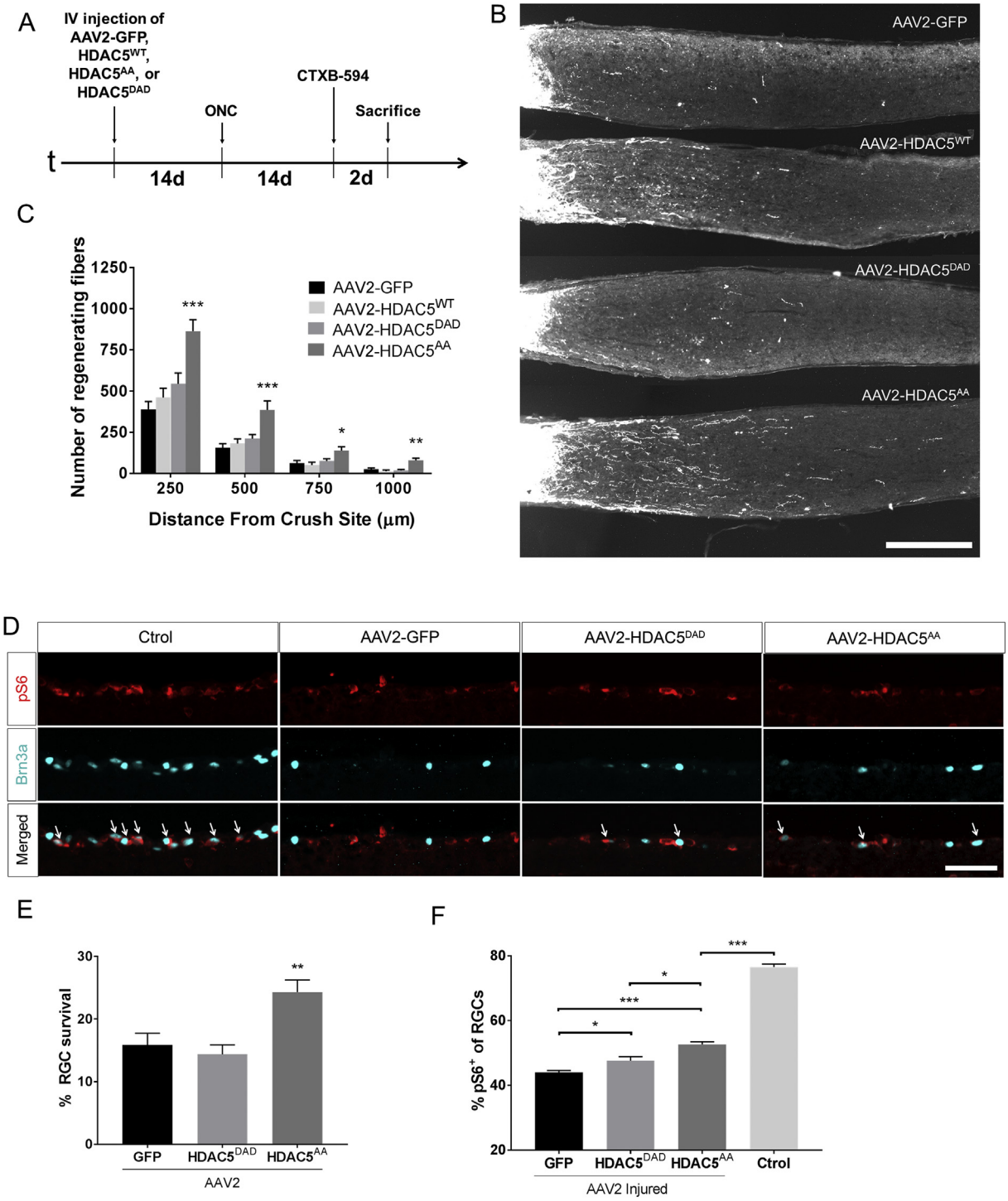

Fig. 3. Overexpression of HDAC5^{AA} but not GFP, HDAC5^{WT}, or HDAC5^{DAD} promotes optic nerve regeneration and RGC survival.
(A) Timeline showing experimental procedures, including intravitreal injection of AAV2-GFP, AAV2-FLAG-HDAC5^{WT}, AAV2-FLAG-HDAC5^{AA}, or AAV2-FLAG-HDAC5^{DAD}, optic nerve crush (ONC), intravitreal injection of Alexa 594 fluorescently labeled cholera toxin b (CTXB-594), and sacrifice of mice. (B) Representative optic nerve sections showing that there are more regenerating axons in retinas infected with AAV2-FLAG-HDAC5^{AA} than in the other conditions. (C) Quantification of (B) showing significant differences in optic nerve transducted with AAV2-FLAG-HDAC5^{AA} compared to other conditions at all distances analyzed. Plotted values in (C) were quantified and expressed as mean ± SEM. One-way ANOVA with Bonferroni post hoc analysis, $^{*}p < .05$, $^{**}p < .01$, $^{***}p < .001$. Scale bar = 250 μm. $N = 20$ for AAV2-GFP, $n = 4$ for AAV2-FLAG-HDAC5^{WT}, $n = 9$ for AAV2-FLAG-HDAC5^{DAD} and $n = 14$ for AAV2-FLAG-HDAC5^{AA}. (D) Retinal sections from mice that were injected with AAV2-GFP, AAV2-FLAG-HDAC5^{AA}, or AAV2-FLAG-HDAC5^{DAD} 15 days prior optic nerve injury and sacrificed 15 days post injury, were stained with Brn3a (nucleus, green, a marker for RGCs) and pS6 (cytoplasm, red, a marker of mTOR activation). The non-injured non-injected contralateral retina was included as Control. Arrows indicate colocalization of both markers. (E) Quantification of the percentage of Brn3a positive cells in injured retinas compared to the non-injured contralateral retina. (F) Quantification of the percentage of pS6^{+}/Brn3a^{+} cells. Plotted values in (B) and (C) were quantified and expressed as mean ± SEM. Statistical Analysis was One-way ANOVA with Tukey's post hoc test. B and D, Scale bar = 500 μm. $N = 5$. (For interpretation of the references to colour in this figure legend, the reader is referred to the web version of this article.)

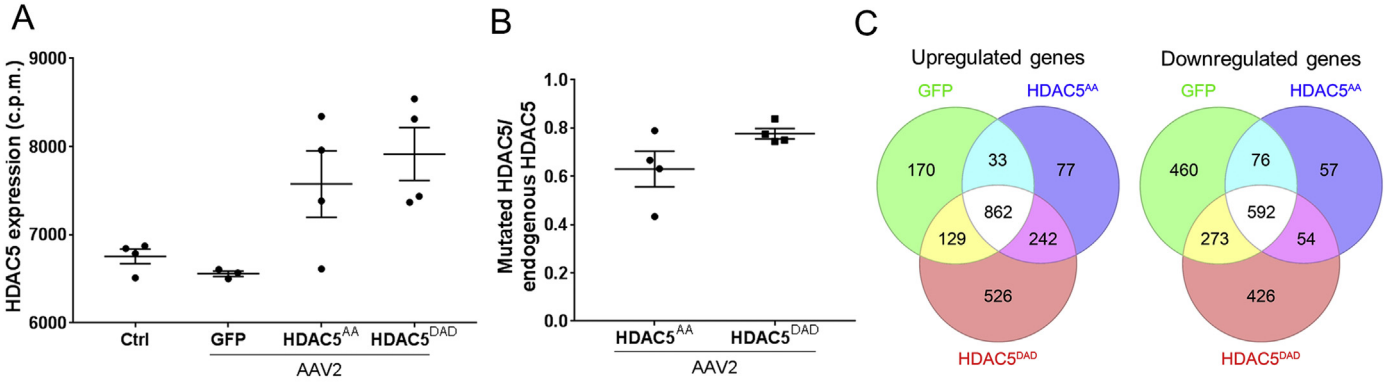

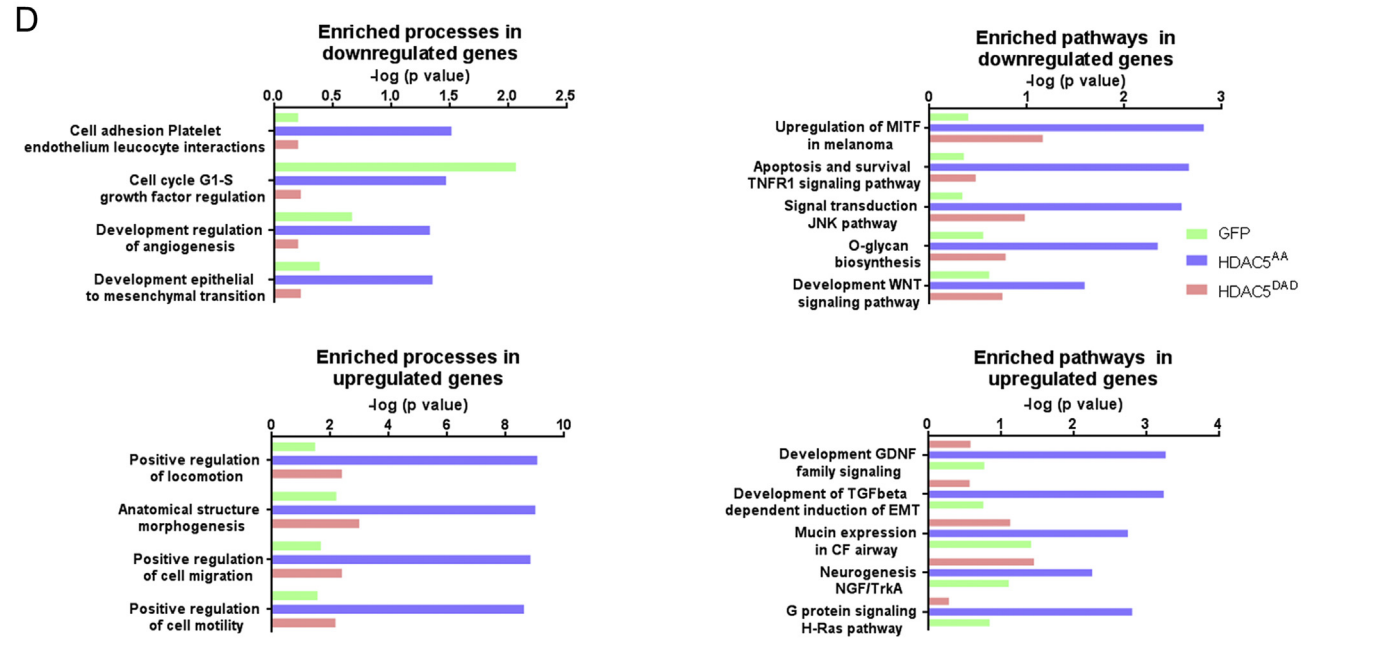

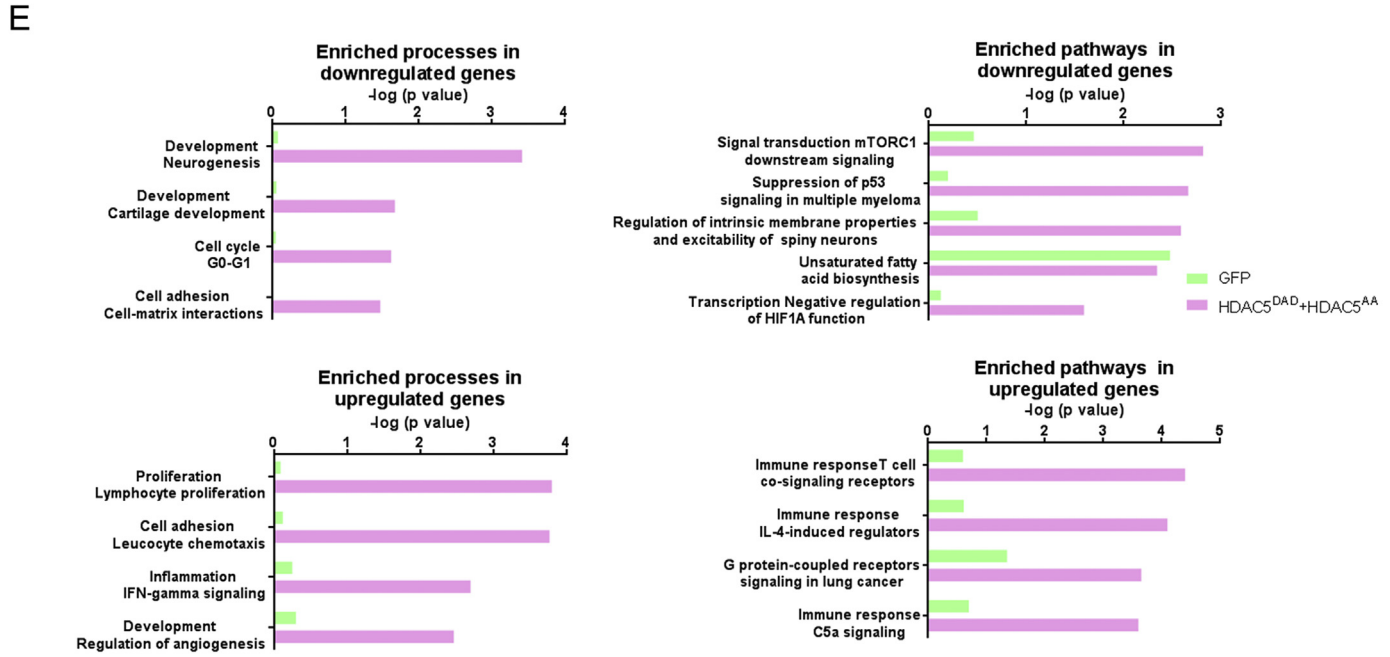

(caption on next page)

Fig. 4. RNAseq analysis demonstrates that HDAC5^{AA} overexpression regulates pathways related to mTOR.
(A) Retinas were intravitreally injected with either AAV2-GFP, AAV2-FLAG-HDAC5^{AA} or AAV2-FLAG-HDAC5^{DAD}. 15 days later, optic nerve injury was performed. 4 days after optic nerve injury, retinas were processed for RNAseq. Control refers to non-injected, non-injured retina. $N = 4$. HDAC5 mRNA expression levels in counts per million (c.p.m) of HDAC5 in the different conditions. (B) Ratio between the number of reads of HDAC5 mutants at the DNA location of serine 498 and number of reads in the homologous region in the endogenous HDAC5. Plotted values in (A) and (B) were quantified and expressed as mean ± SEM. (C) Venn diagram indicating the number of differentially expressed genes in each condition compared to the non-injected, non-injured control retina. (D) Enriched processes and pathways in the set of genes that are differentially expressed in retinas overexpressing GFP, HDAC5^{AA} or HDAC5^{DAD}. (E) Enriched processes and pathways in the set of genes that are differentially expressed in retinas overexpressing GFP compared to both HDAC5^{AA} and HDAC5^{DAD}.

compared to GFP, indicating that these genes are regulated by HDAC5 expression. To determine which pathways and processes are regulated by these specific sets of genes, we performed gene enrichment analysis using MetaCore software (Fig. 4E), which contains a curated knowledge database allowing to obtain functional pathways and processes regulated by defined set of genes. This analysis revealed that the set of genes that are differentially upregulated in retinas overexpressing HDAC5^{AA} relate to “positive regulation of locomotion”, “morphogenesis”, and “cell migration and motility”, which are in line with the effects observed in axon growth (Fig. 4D). Pathways regulated by these set of genes are also known regulators of axon growth and include the “GDNF pathway”; the “TGF-beta pathway”; the “NGF-trkA pathway”; and the “H-Ras pathway” (Fig. 4D). Interestingly, the GDNF pathway (Wang et al., 2007), the TGF beta pathway (Cheng and Hao, 2017), and the NGF-TrkA pathway (Nakamura et al., 2011) directly or indirectly activate the mTOR pathway which has drastic effects on axon regeneration (Park et al., 2008). The set of genes differentially downregulated in retinas overexpressing HDAC5^{AA} compared to HDAC5^{DAD} and GFP did not reveal pathways clearly related with axon growth (Fig. 4D). However, analysis of the genes downregulated in both HDAC5^{DAD} and HDAC5^{AA} (Fig. 4E) revealed pathways related to “development neurogenesis”, “mTORC1 pathway”, and “p53 suppression pathway”. The p53 pathway is known to inhibit mTOR (Feng et al., 2005), suggesting that both HDAC5 mutants impact the mTOR pathway but only HDAC5^{AA} has effects in axon growth.

3.5. The mTOR pathway is necessary and sufficient for HDAC5^{AA} induced axon regeneration

To determine if the mTOR pathway is required for the increased axon regeneration that we observed in RGCs expressing HDAC5^{AA}, we used two different approaches to block mTOR activity in vivo: 1) injecting rapamycin, an mTOR inhibitor (Park et al., 2008) every other day (Fig. 5A, B and C), and 2) deleting the regulatory-associated protein of mTOR (*Raptor)*, which is a necessary binding partner to the mTOR kinase and is required for mTOR function (Hara et al., 2002), by expressing AAV-Cre in the RGC of Raptor floxed mice (Polak et al., 2008) (Fig. 5D, E and F). Both strategies reduced the number of regenerating axons after optic nerve injury to the levels of the control (One-way ANOVA $F(4, 16) = 3.21$, $p = .04$ and $F(4, 4) = 6.05$, $p = .05$ respectively, both with Bonferroni's post hoc test). To test if the decreased axon regeneration observed by inhibiting mTOR results from a decreased survival of RGCs, we measured the number of surviving RGCs. Rapamycin treatment led to a significant increase in the survival of RGCs (Fig. 5C) (One-way ANOVA $F(1, 6) = 43.57$, $p = .0006$), consistent with previous studies (Rodriguez-Muela et al., 2012; Li et al., 2018). In contrast, we observed no difference in RGCs survival by deleting Raptor in RGC (Fig. 5F) (One-way ANOVA $F(1, 8) = 0.4729$, $p = .51$). These results demonstrate that the increased axon regeneration promoted by HDAC5^{AA} requires mTOR activity and is independent of RGC survival.

Next, we expressed HDAC5^{AA} in mice in which the mTOR pathway was genetically activated by deleting its negative regulator TSC2. Overexpressing HDAC5^{AA} and Cre in TSC2 floxed mice (Hernandez et al., 2007) did not increase the number of regenerating axons (One-way ANOVA $F(4, 2) = 6.20$, $p = .14$, with Bonferroni's post hoc test) compared to GFP and Cre controls (Fig. 5E and F). Altogether, these results suggest that the increased axon regeneration observed in RGC expressing HDAC5^{AA} is mediated by the mTOR pathway.

3.6. HDAC5^{AA} synergizes with eye inflammation to stimulate axon regeneration

We next asked whether expression of HDAC5^{AA} in combination with treatments that activate other regenerative pathways different than mTOR further increase axon regeneration. Inducing eye inflammation by injecting zymosan promotes axon regeneration (Leon et al., 2000), and this effect is partially independent of mTOR (Leibinger et al., 2012). We expressed HDAC5^{AA}, and induced inflammation the same day that the optic nerve injury was performed by intravitreally injecting zymosan. We observed that both HDAC5^{AA} alone and zymosan treatment alone promote axon regeneration (Fig. 6A and B). When HDAC5^{AA} was combined with zymosan treatment, an additive effect on axon regeneration was observed at all distances quantified (One-way ANOVA $F(12, 45) = 7.84$, $p = .000001$ with Bonferroni's post hoc test). These results further support the notion that HDAC5^{AA} promotes axon regeneration via mTOR and that these effects can synergize with the pro-regenerative inflammatory responses.

4. Discussion

Our study reveals that HDAC5 is predominantly cytoplasmic in RGCs and its localization is unaffected by injury or manipulation of canonical signaling pathways that regulate transport of class II HDACs between nucleus and cytoplasm. Phosphorylation at serines 259, 280, and 498 are critical for regulating the localization of HDAC5 in cell types such as muscle cells or peripheral nervous system neurons (McKinsey et al., 2000; Ha et al., 2010; Cho et al., 2013). However, our results in RGCs showed a clear cytoplasmic localization of HDAC5 that is unaffected by PKCμ or PKA pathways. Additionally, blocking the CRM1 cytoplasmic transport using leptomycin (Harrison et al., 2004) does not induce HDAC5 nuclear accumulation, suggesting that there is no shuttle of HDAC5 between cytoplasm and nucleus and HDAC5 is for the most part localized in the cytoplasm. The difference between the capacity of HDAC5 to shuttle between cytoplasm and nucleus in PNS neurons and its persistent localization in the cytoplasm of RGCs might be explained by the interaction with different binding partners in each case. These results are also interesting in view of the known interaction between HDAC5 and HDAC3 (Fischle et al., 2002), and the fact that HDAC3 is transported to the nucleus of RGCs after optic nerve injury, turning off many genes in injured RGCs, thereby contributing to promote apoptosis (Pelzel et al., 2010). Our results suggest that HDAC5 is unlikely to modulate the localization of HDAC3 and does not follow HDAC3 to the nucleus. Either these two proteins do not interact in the cytoplasm of RGCs, or HDAC5 interaction with cytoskeletal proteins such as Ankyrin-repeat family proteins, tubulins (McKinsey et al., 2006; Greco et al., 2011; Cho and Cavalli, 2012), or other unidentified proteins sequester HDAC5 in the cytoplasm and prevent HDAC5 of following HDAC3 to the nucleus.

Indeed, beyond subcellular localization, HDAC5 phosphorylation is known to regulate HDAC5 binding with interacting partners (Greco et al., 2011). Our results indicate that HDAC5^{AA} promotes optic nerve

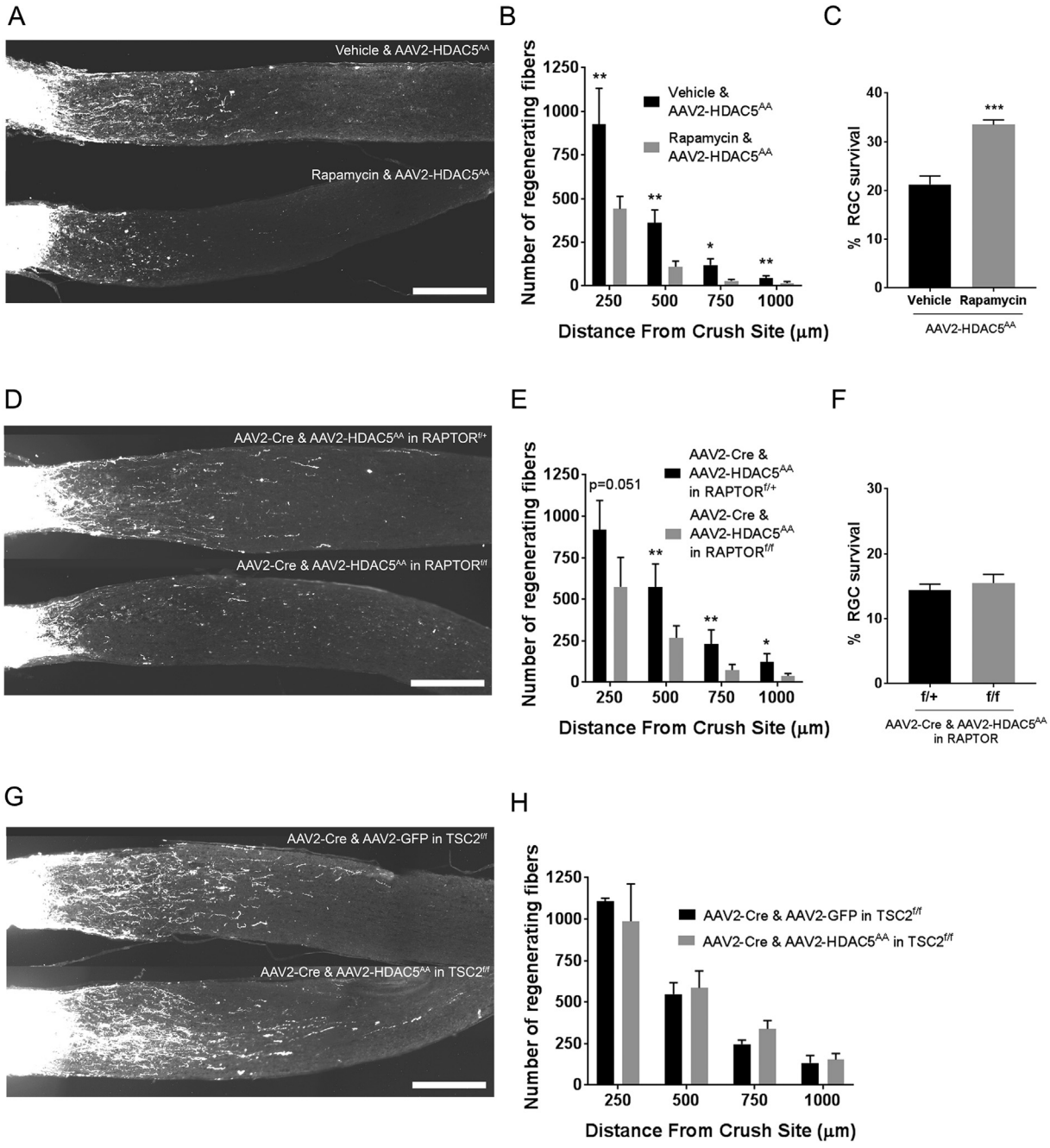

Fig. 5. The mTOR pathway is required for HDAC5^{AA} induced axon regeneration.
(A) Representative optic nerve sections showing axon regeneration in mice that were intravitreally injected with AAV2-FLAG-HDAC5^{AA} 15 days prior injury, and then treated with rapamycin or vehicle until harvest (15 days post optic nerve injury). (B) Quantification of (A) showing that rapamycin injection significantly reduces the number of regenerating axons at all distances analyzed. (C) Quantification of the percentage of Brn3a positive cells in injured retinas of mice treated in (A) compared to the non-injured contralateral retina. (D) Representative optic nerve sections showing axon regeneration in RAPTOR$^{flox/flox}$ or RAPTOR$^{flox/+}$ mice that were injected with AAV2-FLAG-HDAC5^{AA} 15 days prior injury, and with AAV2-Cre 1 day after injection with AAV2-FLAG-HDAC5^{AA}, and sacrificed 15 days post injury. (E) Quantification of (D) showing that RAPTOR deletion in RGCs significantly reduces the number of regenerating axons. (F) Quantification of the percentage of Brn3a positive cells in injured retinas of mice treated in (E) compared to the non-injured contralateral retina. (G) Optic nerve sections collected 15 days after injury from TSC2 $^{flox/flox}$ mice that were injected with either AAV2-FLAG-HDAC5^{AA}, or AAV2-GFP 15 days prior injury, and 1 day after this injection with AAV2-Cre. (H) Quantification of (G) showing that when TSC2 is deleted (leading to mTOR activation), HDAC5^{AA} overexpression is not significantly different than GFP overexpression. Plotted values in (B), (C), (E), (F) and (H) were quantified and expressed as mean ± SEM. Statistical analysis is a One-way ANOVA with Bonferroni's post hoc test in (B), (E) and (H), and a One-way ANOVA with Tukey's post hoc test in (C) and (F), $^{*}p < .05$, $^{**}p < .01$, $^{***}p < .001$. Scale bar = 250 μm. $N = 5$ for vehicle and rapamycin injected mice in (B), $n = 3$ for vehicle and $n = 5$ for rapamycin injected mice in (C), $n = 5$ for RAPTOR$^{flox/+}$ and $n = 6$ for RAPTOR$^{flox/flox}$ in E, $n = 5$ in both conditions of (F), and $n = 4$ and 3 for AAV2-FLAG-HDAC5^{AA} and AAV2-GFP respectively in the TSC2 $^{flox/flox}$ experiment.

regeneration by activating the mTOR pathway in RGCs. There are several experiments in our study that demonstrate that HDAC5^{AA} activates the mTOR pathway to promote optic nerve regeneration. First, axon regeneration induced by HDAC5^{AA} overexpression is prevented by inhibiting the mTOR pathway using rapamycin or by deletion of Raptor, without reducing the number of surviving RGCs.

Interestingly, similar to the control condition, we still observed a number of regenerating axons after blocking mTOR suggesting that

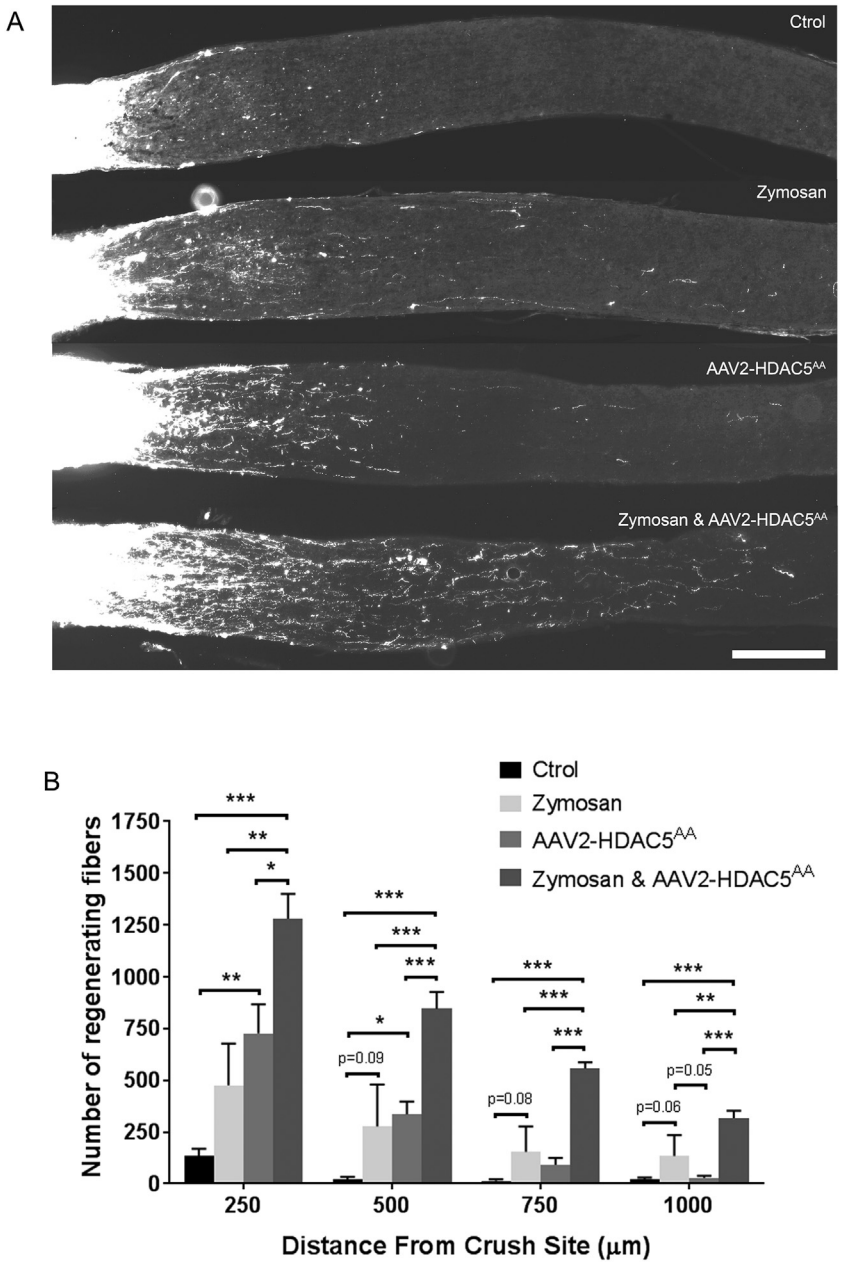

Fig. 6. HDAC5^{AA} overexpression acts additively with an inflammatory stimulus to boost axon regeneration.
(A) Representative optic nerve sections showing axon regeneration in mice that were either untreated, or intravitreally injected with AAV2-FLAG-HDAC5^{AA} 15 days prior injury, injected with zymosan the day of injury, or the combination of these two last treatments. (B) Quantification of (A) showing that the combination of HDAC5^{AA} overexpression and zymosan injection significantly increases the number of regenerating axons at all distances analyzed when compared to the single treatments. Plotted values in (C) were quantified and expressed as mean ± SEM. Statistical analysis is a One-way ANOVA with Bonferroni's post hoc test, $^{*}p < .05$, $^{**}p < .01$, $^{***}p < .001$. Scale bar = 250 µm. $N = 5$ for control, HDAC5^{AA} injected, and zymosan injected, and $n = 7$ for the combination of zymosan injection and HDAC5^{AA} overexpression.

blocking mTOR pathway does not indiscriminately block all regeneration. Indeed, a previous study demonstrated that although rapamycin reduces the number of regenerating axons at long distances from the injury site (1000 µm) in response to an inflammatory stimulus applied to the retina, it does not affect the number of regenerating axons at short distances (500 µm) (Leibinger et al., 2012). Moreover, this study also showed that purified RGCs stimulated with CNTF grow axons at the same rate when the mTOR pathway is inhibited with rapamycin (Leibinger et al., 2012).

Our study also reveals that applying an inflammatory stimulus by intravitreally injecting zymosan does have an additive effect with HDAC5^{AA}. In contrast, deleting TSC2, which activates the mTOR pathway, does not have an additive effect, emphasizing the link between HDAC5^{AA} overexpression and mTOR activation.

Whereas activation of mTOR by PTEN deletion completely reverts the decrease in pS6 staining produced by injury (Park et al., 2008), our data show that HDAC5^{AA} reverts part of the pS6 decay after injury, suggesting that even with a modest activation of mTOR, a substantial axon regeneration can be achieved. However, a direct comparison between these studies is difficult because of the different antibodies used. Whereas we used an antibody that recognizes the phosphorylated serine 240/244, Park et al. used an antibody that recognizes phosphorylated serine 235/236 (Park et al., 2008). Both phosphorylation sites are phosphorylated by pS6 kinase, which is activated by mTOR. However, serine p240/244 is a more reliable marker of pS6 kinase activation since it is exclusively phosphorylated by pS6 kinase while p235/236 is also phosphorylated by other kinases (Roux et al., 2007). Of note, it has been previously shown that CNS neurons have a higher phosphorylation at serine 240/244 compared to serine 235/236 (Liu et al., 2014), which may explain the higher number of pS6 positive RGCs observed in our study compared to others studies.

It is also noteworthy that blocking mTOR activity in RGCs overexpressing HDAC5^{AA} did not reduce their survival. Other studies reported that the increase in surviving RGCs mediated by PTEN deletion is prevented by rapamycin treatment (Park et al., 2008). We found that rapamycin treatment in HDAC5^{AA} expressing mice increased RGC survival. The neuroprotective effect of rapamycin is suggested to occur through either an inhibition of retinal gliosis (Li et al., 2018) or an

activation of autophagy (Rodriguez-Muela et al., 2012). Since, rapamycin treatment can increase or decrease survival depending on the context, it might be difficult to tease apart the two mechanisms in our experiment, especially considering that, the increase of RGC survival mediated by rapamycin (Rodriguez-Muela et al., 2012), and the increase mediated by $HDAC5^{AA}$ are relatively modest compared to the PTEN deletion (Park et al., 2008). Interestingly, blocking mTOR by Raptor deletion did not reduce the number of surviving RGCs, suggesting that the increase in survival mediated by $HDAC5^{AA}$ is caused by an mTOR independent mechanism, or that $HDAC5^{AA}$ overexpression does not increase survival in the Raptor floxed mouse background.

The exact mechanism by which $HDAC5^{AA}$ activates the mTOR pathway in RGC remains to be elucidated. There is evidence in a hypothalamic cell line that HDAC5 interacts and deacetylates Raptor, thereby activating mTOR (Ma et al., 2015). A similar mechanism might be taking place in RGCs. Both $HDAC5^{DAD}$ and $HDAC5^{AA}$ are able to activate mTOR pathway according to the pS6 staining in injured retinas and the RNAseq pathway analysis. However, these same results also showed that $HDAC5^{AA}$ is more effective in activating mTOR and probably for this reason is the only one that significantly promotes axon regeneration. It is possible that $HDAC5^{AA}$ has more affinity for Raptor compared to $HDAC5^{DAD}$ and therefore favors its deacetylation. Indeed, HDAC5 phosphorylation is known to regulate HDAC5 binding with interacting partners (Greco et al., 2011). Another possibility is that $HDAC5^{AA}$ activates the expression of pro-growth genes in the nucleus that leads to the activation of the mTOR pathway, since our RNAseq data reveals that both HDAC5 mutants can regulate mTOR by regulating the expression of genes in the mTORC1 pathway or in the p53 pathway (Feng et al., 2005). Similarly, deletion of class I histone deacetylases HDAC1 and HDAC2 in RGCs induce a downregulation of p53 and promotes RGCs survival (Lebrun-Julien and Suter, 2015). These results suggest that activation of mTOR by $HDAC5^{AA}$ regulates directly or indirectly signaling pathways that establish a pro-growth program. However, our RNAseq analysis used whole retina and other cell types, such as reactive glia, might also contribute to the observed difference in gene expression. Future studies will be required to confirm these hypotheses.

In conclusion, our study demonstrates that HDAC5 is largely localized in the cytoplasm of RGC and is unaffected by the manipulation of PKCμ, PKA, or even the inhibition of nuclear export. It further demonstrates that blocking the phosphorylation of HDAC5 at serine 259 and 498 by substitution with alanine does not induce nuclear localization, but partially prevents the decline in mTOR activity caused by injury (Park et al., 2008) and promotes optic nerve regeneration and RGCs survival. Our results suggest a new therapeutic target for future studies that aim to promote axon regeneration through mTOR activation.

Acknowledgements

This work was supported in part by National Institutes of Health Grants EY029077, NS082446 and NS096034 (to V.C.), a Philip and Sima K. Needleman Doctoral Fellowship (to M.M) and a BioSURF fellowship (to A.J). We would like to thank the Hope Center Viral Vectors Core at Washington University School of Medicine for generating the AAV virus, the Genome Technology Access Center at Washington University for performing the RNA sequencing, Guoyan Zhao for help with HDAC5 expression analysis in the RNAseq data, Alan Sang for technical assistance and Amber Hackett for her constructive comments on the manuscript.

Conflict of interest statement

The authors declare no conflict of interest.

References

Abe, N., Borson, S.H., Gambello, M.J., Wang, F., Cavalli, V., 2010. Mammalian target of rapamycin (mTOR) activation increases axonal growth capacity of injured peripheral nerves. J. Biol. Chem. 285, 28034–28043.
Ban, N., Siegfried, C.J., Lin, J.B., Shui, Y.B., Sein, J., Pita-Thomas, W., Sene, A., Santeford, A., Gordon, M., Lamb, R., Dong, Z., Kelly, S.C., Cavalli, V., Yoshino, J., Apte, R.S., 2017. GDF15 is elevated in mice following retinal ganglion cell death and in glaucoma patients. JCI Insight 2.
Barres, B.A., Silverstein, B.E., Corey, D.P., Chun, L.L., 1988. Immunological, morphological, and electrophysiological variation among retinal ganglion cells purified by panning. Neuron 1, 791–803.
Berry, M., Ahmed, Z., Logan, A., 2019. Return of function after CNS axon regeneration: lessons from injury-responsive intrinsically photosensitive and alpha retinal ganglion cells. Prog. Retin. Eye Res (In Press, Available online 17 November 2018).
Chen, C., Liu, Y., Liu, Y., Zheng, P., 2009. mTOR regulation and therapeutic rejuvenation of aging hematopoietic stem cells. Sci. Signal. 2, ra75.
Cheng, K.Y., Hao, M., 2017. Mammalian target of rapamycin (mTOR) regulates transforming growth factor-beta1 (TGF-beta1)-induced epithelial-mesenchymal transition via decreased pyruvate kinase M2 (PKM2) expression in cervical cancer cells. Med. Sci. Monit. 23, 2017–2028.
Cho, Y., Cavalli, V., 2012. HDAC5 is a novel injury-regulated tubulin deacetylase controlling axon regeneration. EMBO J. 31, 3063–3078.
Cho, Y., Sloutsky, R., Naegle, K.M., Cavalli, V., 2013. Injury-induced HDAC5 nuclear export is essential for axon regeneration. Cell 155, 894–908.
Christie, K.J., Webber, C.A., Martinez, J.A., Singh, B., Zochodne, D.W., 2010. PTEN inhibition to facilitate intrinsic regenerative outgrowth of adult peripheral axons. J. Neurosci. 30, 9306–9315.
de Lima, S., Koriyama, Y., Kurimoto, T., Oliveira, J.T., Yin, Y., Li, Y., Gilbert, H.Y., Fagiolini, M., Martinez, A.M., Benowitz, L., 2012. Full-length axon regeneration in the adult mouse optic nerve and partial recovery of simple visual behaviors. Proc. Natl. Acad. Sci. U. S. A. 109, 9149–9154.
Duan, X., Qiao, M., Bei, F., Kim, I.J., He, Z., Sanes, J.R., 2015. Subtype-specific regeneration of retinal ganglion cells following axotomy: effects of osteopontin and mTOR signaling. Neuron 85, 1244–1256.
Feng, Z., Zhang, H., Levine, A.J., Jin, S., 2005. The coordinate regulation of the p53 and mTOR pathways in cells. Proc. Natl. Acad. Sci. U. S. A. 102, 8204–8209.
Fischle, W., Dequiedt, F., Hendzel, M.J., Guenther, M.G., Lazar, M.A., Voelter, W., Verdin, E., 2002. Enzymatic activity associated with class II HDACs is dependent on a multiprotein complex containing HDAC3 and SMRT/N-CoR. Mol. Cell 9, 45–57.
Gaub, P., Joshi, Y., Wuttke, A., Naumann, U., Schnichels, S., Heiduschka, P., Di Giovanni, S., 2011. The histone acetyltransferase p300 promotes intrinsic axonal regeneration. Brain 134, 2134–2148.
Gray, J.T., Zolotukhin, S., 2011. Design and construction of functional AAV vectors. Methods Mol. Biol. 807, 25–46.
Greco, T.M., Yu, F., Guise, A.J., Cristea, I.M., 2011. Nuclear import of histone deacetylase 5 by requisite nuclear localization signal phosphorylation. Mol. Cell. Proteomics 10 (M110), 004317.
Ha, C.H., Kim, J.Y., Zhao, J., Wang, W., Jhun, B.S., Wong, C., Jin, Z.G., 2010. PKA phosphorylates histone deacetylase 5 and prevents its nuclear export, leading to the inhibition of gene transcription and cardiomyocyte hypertrophy. Proc. Natl. Acad. Sci. U. S. A. 107, 15467–15472.
Hara, K., Maruki, Y., Long, X., Yoshino, K., Oshiro, N., Hidayat, S., Tokunaga, C., Avruch, J., Yonezawa, K., 2002. Raptor, a binding partner of target of rapamycin (TOR), mediates TOR action. Cell 110, 177–189.
Harrison, B.C., Roberts, C.R., Hood, D.B., Sweeney, M., Gould, J.M., Bush, E.W., McKinsey, T.A., 2004. The CRM1 nuclear export receptor controls pathological cardiac gene expression. Mol. Cell. Biol. 24, 10636–10649.
Harvey, A.R., Kamphuis, W., Eggers, R., Symons, N.A., Blits, B., Niclou, S., Boer, G.J., Verhaagen, J., 2002. Intravitreal injection of adeno-associated viral vectors results in the transduction of different types of retinal neurons in neonatal and adult rats: a comparison with lentiviral vectors. Mol. Cell. Neurosci. 21, 141–157.
Hernandez, O., Way, S., McKenna 3rd, J., Gambello, M.J., 2007. Generation of a conditional disruption of the Tsc2 gene. Genesis 45, 101–106.
Iglesias, T., Rozengurt, E., 1998. Protein kinase D activation by mutations within its pleckstrin homology domain. J. Biol. Chem. 273, 410–416.
Lebrun-Julien, F., Suter, U., 2015. Combined HDAC1 and HDAC2 depletion promotes retinal ganglion cell survival after injury through reduction of p53 target gene expression. ASN Neuro 7.
Leibinger, M., Andreadaki, A., Fischer, D., 2012. Role of mTOR in neuroprotection and axon regeneration after inflammatory stimulation. Neurobiol. Dis. 46, 314–324.
Leon, S., Yin, Y., Nguyen, J., Irwin, N., Benowitz, L.I., 2000. Lens injury stimulates axon regeneration in the mature rat optic nerve. J. Neurosci. 20, 4615–4626.
Li, S., Yang, C., Zhang, L., Gao, X., Wang, X., Liu, W., Wang, Y., Jiang, S., Wong, Y.H., Zhang, Y., Liu, K., 2016. Promoting axon regeneration in the adult CNS by modulation of the melanopsin/GPCR signaling. Proc. Natl. Acad. Sci. U. S. A. 113, 1937–1942.
Li, N., Wang, F., Zhang, Q., Jin, M., Lu, Y., Chen, S., Guo, C., Zhang, X., 2018. Rapamycin mediates mTOR signaling in reactive astrocytes and reduces retinal ganglion cell loss. Exp. Eye Res. 176, 10–19.
Liu, Y., Contreras, M., Shen, T., Randall, W.R., Schneider, M.F., 2009. Alpha-adrenergic signalling activates protein kinase D and causes nuclear efflux of the transcriptional repressor HDAC5 in cultured adult mouse soleus skeletal muscle fibres. J. Physiol. 587, 1101–1115.
Liu, J., Reeves, C., Michalak, Z., Coppola, A., Diehl, B., Sisodiya, S.M., Thom, M., 2014.

Evidence for mTOR pathway activation in a spectrum of epilepsy-associated pathologies. Acta Neuropathol. Commun. 2, 71.
Ma, L., Tang, H., Yin, Y., Yu, R., Zhao, J., Li, Y., Mulholland, M.W., Zhang, W., 2015. HDAC5-mTORC1 interaction in differential regulation of ghrelin and nucleobindin 2 (NUCB2)/Nesfatin-1. Mol. Endocrinol. 29, 1571–1580.
Mahar, M., Cavalli, V., 2018. Intrinsic mechanisms of neuronal axon regeneration. Nat. Rev. Neurosci. 19, 323–337.
McKinsey, T.A., Zhang, C.L., Lu, J., Olson, E.N., 2000. Signal-dependent nuclear export of a histone deacetylase regulates muscle differentiation. Nature 408, 106–111.
McKinsey, T.A., Kuwahara, K., Bezprozvannaya, S., Olson, E.N., 2006. Class II histone deacetylases confer signal responsiveness to the ankyrin-repeat proteins ANKRA2 and RFXANK. Mol. Biol. Cell 17, 438–447.
Nakamura, K., Tan, F., Li, Z., Thiele, C.J., 2011. NGF activation of TrkA induces vascular endothelial growth factor expression via induction of hypoxia-inducible factor-1alpha. Mol. Cell. Neurosci. 46, 498–506.
Park, K.K., Liu, K., Hu, Y., Smith, P.D., Wang, C., Cai, B., Xu, B., Connolly, L., Kramvis, I., Sahin, M., He, Z., 2008. Promoting axon regeneration in the adult CNS by modulation of the PTEN/mTOR pathway. Science 322, 963–966.
Pasut, A., Jones, A.E., Rudnicki, M.A., 2013. Isolation and culture of individual myofibers and their satellite cells from adult skeletal muscle. J. Vis. Exp. 73, e50074.
Pelzel, H.R., Schlamp, C.L., Nickells, R.W., 2010. Histone H4 deacetylation plays a critical role in early gene silencing during neuronal apoptosis. BMC Neurosci. 11, 62.
Polak, P., Cybulski, N., Feige, J.N., Auwerx, J., Ruegg, M.A., Hall, M.N., 2008. Adipose-specific knockout of raptor results in lean mice with enhanced mitochondrial respiration. Cell Metab. 8, 399–410.
Quigley, H.A., 2016. Understanding glaucomatous optic neuropathy: the synergy between clinical observation and investigation. Annu. Rev. Vis. Sci. 2, 235–254.
Rodriguez-Muela, N., Germain, F., Marino, G., Fitze, P.S., Boya, P., 2012. Autophagy promotes survival of retinal ganglion cells after optic nerve axotomy in mice. Cell Death Differ. 19, 162–169.
Roux, P.P., Shahbazian, D., Vu, H., Holz, M.K., Cohen, M.S., Taunton, J., Sonenberg, N., Blenis, J., 2007. RAS/ERK signaling promotes site-specific ribosomal protein S6 phosphorylation via RSK and stimulates cap-dependent translation. J. Biol. Chem. 282, 14056–14064.
Schmitt, H.M., Pelzel, H.R., Schlamp, C.L., Nickells, R.W., 2014. Histone deacetylase 3 (HDAC3) plays an important role in retinal ganglion cell death after acute optic nerve injury. Mol. Neurodegener. 9, 39.
Schmitt, H.M., Schlamp, C.L., Nickells, R.W., 2018. Targeting HDAC3 activity with RGFP966 protects against retinal ganglion cell nuclear atrophy and apoptosis after optic nerve injury. J. Ocul. Pharmacol. Ther. 34, 260–273.
SR, C., 1913. Degeneration and Regeneration of the Nervous System. Oxford University Press.
Steketee, M.B., Goldberg, J.L., 2012. Signaling endosomes and growth cone motility in axon regeneration. Int. Rev. Neurobiol. 106, 35–73.
Trakhtenberg, E.F., Pita-Thomas, W., Fernandez, S.G., Patel, K.H., Venugopalan, P., Shechter, J.M., Morkin, M.I., Galvao, J., Liu, X., Dombrowski, S.M., Goldberg, J.L., 2017. Serotonin receptor 2C regulates neurite growth and is necessary for normal retinal processing of visual information. Dev. Neurobiol. 77, 419–437.
Vega, R.B., Harrison, B.C., Meadows, E., Roberts, C.R., Papst, P.J., Olson, E.N., McKinsey, T.A., 2004. Protein kinases C and D mediate agonist-dependent cardiac hypertrophy through nuclear export of histone deacetylase 5. Mol. Cell. Biol. 24, 8374–8385.
Wang, H.J., Cao, J.P., Yu, J.K., Gao, D.S., 2007. Role of PI3-K/Akt pathway and its effect on glial cell line-derived neurotrophic factor in midbrain dopamine cells. Acta Pharmacol. Sin. 28, 166–172.
Xie, C., Lu, H., Nomura, A., Hanse, E.A., Forster, C.L., Parker, J.B., Linden, M.A., Karasch, C., Hallstrom, T.C., 2015. Co-deleting Pten with Rb in retinal progenitor cells in mice results in fully penetrant bilateral retinoblastomas. Mol. Cancer 14, 93.
Yin, Y., Cui, Q., Li, Y., Irwin, N., Fischer, D., Harvey, A.R., Benowitz, L.I., 2003. Macrophage-derived factors stimulate optic nerve regeneration. J. Neurosci. 23, 2284–2293.